# AORTIC STENOSIS AND SYSTEMIC HYPERTENSION, MODELING OF

DAMIEN GARCIA
LOUIS-GILLES DURAND
Institut de Recherches Cliniques de Montréal
Montreal, Canada

## 1. INTRODUCTION

Aortic stenosis (AS) is the most common cardiovascular disease after hypertension and coronary artery disease and is the most frequent cause of valvular replacement in developed countries (1,2). This disease refers to the narrowing of the aortic valve opening during left ventricular (LV) ejection (Fig. 1a). This can be caused by a congenital abnormality of the valve (for example, the valve could have only two cusps instead of three). The most common cause of AS today is, however, the calcification of the valve cusps induced by a progressive degeneration of leaflet tissue (senile degenerative stenosis) (3). The narrowing of the valve aperture induces an obstruction to blood flow from the left ventricle to the aorta resulting in an increase in LV afterload (Fig. 1b). When AS becomes severe, symptoms such as shortness of breath, chest pain, and dizziness may occur and survival is markedly reduced (3). Once patients develop symptoms, prompt aortic valve replacement is generally needed. In patients with AS, the prevalence of systemic hypertension ranges from 30 to 40 % (4,5).

Systemic hypertension (HPT) is due to abnormally high blood pressure in the systemic arteries, i.e., in the vessels that carry blood from the heart to the organs. It is generally brought on by two interrelated physiological factors (6): (1) a reduction in the caliber of small arteries or arterioles with an ensuing increase in systemic vascular resistance and mean blood pressure, and (2) a reduction in the arterial compliance (ability of an artery to distend with increasing transmural pressure) with a resulting increase in pulse pressure (systolic minus diastolic blood pressure). When AS coexists with HPT, the left ventricle faces a double pressure overload (valvular and vascular). Consequently, symptoms of AS develop at a lesser degree of valvular obstruction in hypertensive compared with normotensive patients (4). In the presence of AS and/or HPT, a compensatory concentric hypertrophy of the left ventricle appears which contributes to preserve an adequate cardiac performance. Concentric hypertrophy is primarily characterized by an LV wall thickening, as new contractile-protein units are generated in parallel to the existing ones, whereas the LV cavity volume generally remains unchanged (Fig. 1b). It thus compensates for the increased LV wall stress and tends to maintain a normal cardiac output (7,8). In the clinical situation of coexistent valvular and vascular overloads, it is difficult to differentiate the events caused by AS from those caused by HPT. A detailed understanding of the respective impacts of AS and HPT on the LV function would help to predict whether aortic valve replacement and/or antihypertensive medical treatment would be beneficial in this particular situation. It is, however, difficult to perform a comprehensive analysis of the interaction between different pathologies in the context of a clinical study because this approach usually requires a large number of physiological measurements in a large cohort of patients. In addition, these measurements are often difficult to achieve, if at all

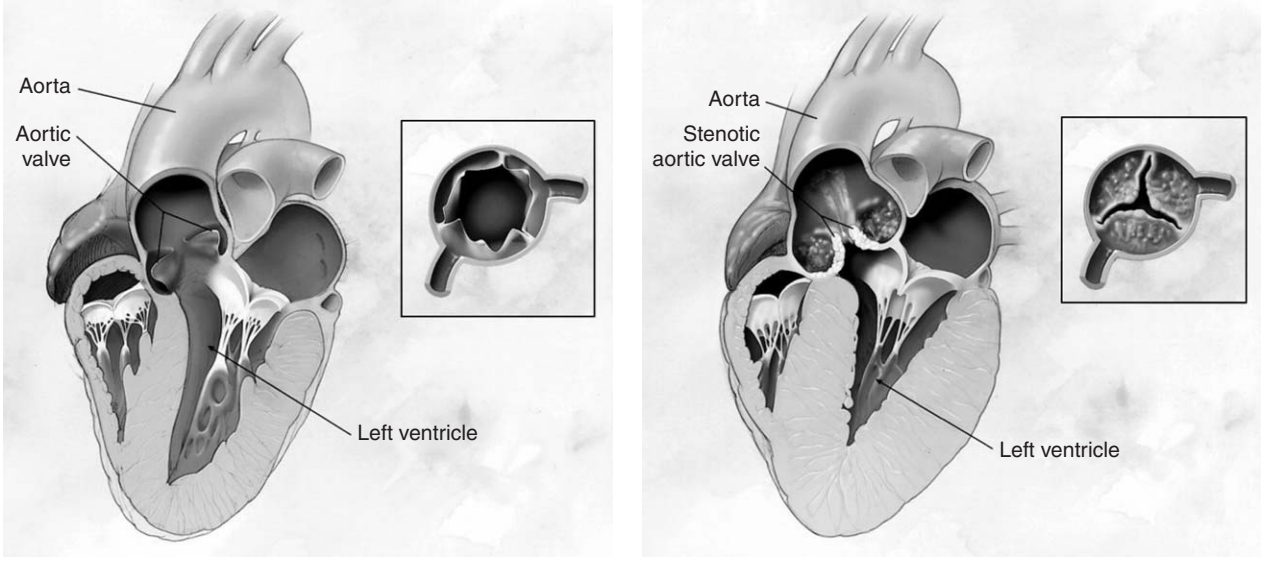


**Figure 1.** Schema of the heart during ejection. (a) without aortic stenosis, the aortic valve is fully opened; (b) in the presence of aortic stenosis, the calcified aortic valve cannot open fully, which causes an obstruction to blood flow from the left ventricle to the aorta and produces a transvalvular flow jet. Note the increase in left ventricular wall thickness. From Nishimura (3) with permission.



*Wiley Encyclopedia of Biomedical Engineering,* Copyright © 2006 John Wiley & Sons, Inc.

possible, in patients. The use of mathematical or numerical models may overcome this dilemma.

Several theoretical cardiovascular models have been proposed to analyze the effect of vascular properties and/or AS on the LV function (9–17). Most of these models contain, however, numerous independent input parameters so that their potential application in the clinical setting may be very limited. Moreover, only a few numerical models include the effect of AS (11,12,14). But these latter assume a linear relationship between the transvalvular flow rate and the pressure difference across the AS. Such a representation is inaccurate since the flow-pressure relationship in AS is by far non-linear. To overcome these limitations, we thus developed an explicit analytical representation of the AS hemodynamics (18), which was incorporated in a simple cardiovascular model based on the so-called three-element windkessel model (19). The resulting ventricular-valvular-vascular mathematical model ($V^3$ model) and its main features will be depicted in this chapter. In the next section, we first describe the AS hemodynamics and the inherent hypotheses used for the derivation of the corresponding analytical model. The ventricular and the vascular models are then briefly explained before introducing the $V^3$ model. We then describe some findings obtained with the numerical $V^3$ model and their clinical implications. We finally conclude by presenting potential future improvements of the mathematical $V^3$ model.

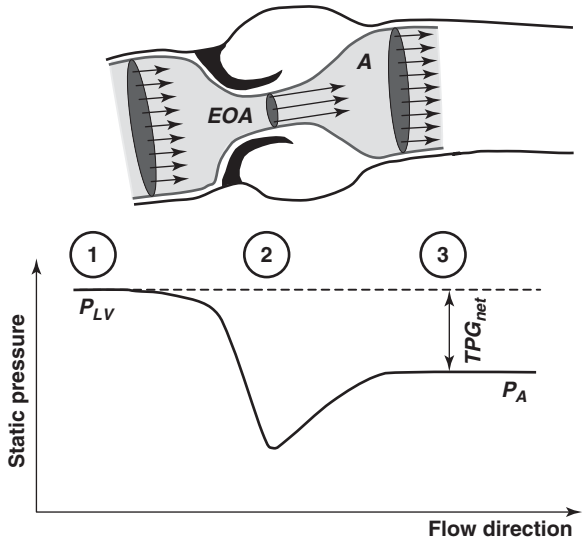


**Figure 2.** Schema of the flow across an aortic valve during systole and corresponding pressure field along the flow axis. Locations 1, 2, and 3 correspond to the detachment of the flow from the left ventricular outflow tract, the vena contracta, and the location where pressure is recovered. $TPG_{net}$ is the net transvalvular pressure gradient and *EOA* is the valvular effective orifice area. $P_{LV}$ = left ventricular pressure, $P_A$ = aortic pressure, $A$ = cross-sectional area of the ascending aorta.

## 2. THEORETICAL MODELS

### 2.1. Description of the Flow across the Aortic Stenosis

For convenience, we define left ventricular (LV) systole as the LV ejection period, i.e., the period where the transvalvular flow rate ($Q$) is strictly positive. The flow pattern across an aortic stenosis (AS) is very similar to the one occurring in orifice plates used as differential-pressure flow metering devices (20). It is mainly characterized by a flow contraction as far as the vena contracta, followed by an abrupt expansion (Fig. 2). The vena contracta corresponds to the location where the cross-sectional area of the jet is minimal (location 2, Fig. 2). This area is called the effective orifice area (*EOA*) of the valve. Within the contraction region, upstream from the vena contracta, some static pressure is converted to dynamic pressure. Flow contraction is a stable process with virtually no energy loss (21). Beyond the vena contracta, the fluid decelerates as the area occupied by the throughflow increases to fill the cross-section of the ascending aorta. The jet is rapidly lost in a region of turbulent mixing which involves significant fluid energy dissipation. In this region, the static pressure increases until it reaches a maximum beyond the location where the reattachment of the flow occurs. The difference between LV pressure and recovered aortic pressure is called the net transvalvular pressure gradient (location 3, Fig. 2) or $TPG_{net}$ (22). Note that cardiologists rather use the expression "pressure gradient" where a physicist would properly utilize "pressure difference," reserving the term "gradient" to express the rate of change in pressure per unit distance (23). To remain consistent with the clinical terminology, the term "pressure gradient" will be used in this chapter. The following section thoroughly describes the theoretical development of the instantaneous $TPG_{net}$ expression as a function of transvalvular flow rate ($Q$) and effective orifice area (*EOA*). The mathematical derivation is adapted with permission from our previous work (18).

### 2.2. The Pessure-Flow Relationship in Aortic Stenosis

According to the aforementioned properties of the transvalvular flow, we first suppose that the fluid is ideal (i.e., incompressible and nonviscous) upstream from the vena contracta. Second, we postulate that the valve opens and closes instantaneously and that its *EOA* remains constant throughout systole. Third, we assume that the velocity profiles are flat (plug flow) within the throughflow. Finally, for simplicity's sake, we suppose that the respective cross-sectional areas of the LV outflow tract (upstream section, location 1, Fig. 2) and of the ascending aorta (downstream section, location 3, Fig. 2) are equal and noted $A$.

Because gravitation has no significant effect on the transvalvular flow and blood is an incompressible fluid, the generalized Bernoulli equation used along the axial streamline linking LV outflow tract (location 1) with ascending aorta (location 3) yields $TPG_{net}$:

$$TPG_{net} = P_{LV} - P_A = P_1 - P_3 = \frac{1}{2}\rho\left(U_3^2 - U_1^2\right) + \rho\int_1^3 \frac{\partial U}{\partial t}\,\mathrm{d}l + E_L \qquad (1)$$

where $P$, $U$ and $\rho$ are the pressure, the velocity, and the

density of the fluid, respectively. Coordinate $l$ is the curvilinear coordinate along the considered streamline and the subscripts refer to the location number. $E_L$ is the total energy loss induced by the flow expansion. Because the cross-sectional areas are similar in locations 1 and 3 and velocity profiles are flat, $U_1 = U_3$. Therefore,

$$TPG_{net} = \rho \int_1^3 \frac{\partial U}{\partial t} \mathrm{d}l + E_L \tag{2}$$

According to the conservation of mass, the transvalvular flow rate $Q$ can be written as $Q = A(l)U(l)$, where $A(l)$ is the cross-sectional area of the through-flow at location $l$. If we further assume that $A(l)$ is not time-dependent, Equation 2 therefore yields

$$TPG_{net} = \rho \frac{\partial Q}{\partial t} \int_1^3 \frac{1}{A(l)} \mathrm{d}l + E_L \tag{3}$$

To obtain the complete expression of $TPG_{net}$, one has to know $E_L$. Recalling that no energy loss occurs upstream from the vena contracta, $E_L$ appears in the generalized Bernoulli equation applied between locations 2 and 3:

$$P_2 - P_3 = \frac{1}{2}\rho\left(U_3^2 - U_2^2\right) + \rho \int_2^3 \frac{\partial U}{\partial t} \mathrm{d}l + E_L \tag{4}$$

Using the mass conservation, as above, this can be rewritten as

$$P_2 - P_3 = \frac{1}{2}\rho Q^2 \left(\frac{1}{A^2} - \frac{1}{EOA^2}\right) + \rho \frac{\partial Q}{\partial t} \int_2^3 \frac{1}{A(l)} \mathrm{d}l + E_L \tag{5}$$

For a control volume $\Omega$ that is fixed and non-deforming and whose boundary is noted $\Gamma$, Newton's second law of motion applied to an incompressible flow can be written as (24)

$$\rho \int_\Omega \frac{\partial U}{\partial t} \mathrm{d}\Omega + \rho \int_\Gamma U U \cdot n \mathrm{d}\Gamma = \sum F \tag{6}$$

where $\boldsymbol{U}$ is the fluid velocity vector, $\boldsymbol{n}$ is the outward-pointing normal, and $\boldsymbol{F}$ are the forces that act on what is contained in $\Omega$. Let's consider the fluid contained in the control volume $\Omega$ delimited by the aortic wall and the respective cross-sections at location 2 and location 3 (Fig. 2). Since the action of gravity and the wall shear forces are negligible here, the only axial forces acting on the fluid contained in $\Omega$ are the inlet and outlet pressure forces. Because velocities are uniform in locations 2 and 3, it follows from Equation 6 applied to $\Omega$:

$$\rho \int_\Omega \frac{\partial U}{\partial t} \mathrm{d}\Omega - \rho U_2^2 EOA + \rho U_3^2 A = (P_2 - P_3)A \tag{7}$$

Again, the conservation of mass leads to

$$\rho \int_2^3 \frac{\partial Q}{\partial t} \mathrm{d}l + \rho Q^2 \left(\frac{1}{A} - \frac{1}{EOA}\right) = (P_2 - P_3)A \tag{8}$$

From the combination of Equations 5 and 8, one can get the energy loss:

$$E_L = \rho \frac{\partial Q}{\partial t} \left(\frac{1}{A}\int_2^3 \mathrm{d}l - \int_2^3 \frac{1}{A(l)} \mathrm{d}l\right) + \frac{1}{2}\rho Q^2 \left(\frac{1}{EOA} - \frac{1}{A}\right)^2 \tag{9}$$

Finally, Equations 2, 9 give the expression of $TPG_{net}$:

$$TPG_{net} = \rho \frac{\partial Q}{\partial t} \left(\frac{L_{23}}{A} + \int_1^2 \frac{1}{A(l)} \mathrm{d}l\right) + \frac{1}{2}\rho Q^2 \left(\frac{1}{EOA} - \frac{1}{A}\right)^2 \tag{10}$$

where $L_{23} = \int_2^3 \mathrm{d}l$ is the recovery length, i.e., the distance separating the vena contracta (location 2, Fig. 2) from the location where static pressure is totally recovered (location 3, Fig. 2). As shown by Equation 10, $TPG_{net}$ is governed by the local inertia (involving $\partial Q/\partial t$) and by the convective inertia (involving $Q^2$). The first term in brackets, related to the local inertia, is purely associated to the geometry of the flow jet and is homogeneous to the inverse of a length. We therefore define the parameter $\lambda$, homogeneous to a length, as follows:

$$\frac{1}{\lambda} = \frac{L_{23}}{A} + \int_1^2 \frac{1}{A(l)} \mathrm{d}l \tag{11}$$

so that Equation 10 is reduced to

$$TPG_{net} = \rho \frac{1}{\lambda}\frac{\partial Q}{\partial t} + \frac{1}{2}\rho Q^2 \left(\frac{1}{EOA} - \frac{1}{A}\right)^2 \tag{12}$$

It can be noticed from Equation 11 that when $EOA$ [i.e., $A(l=2)$] converges toward zero, $1/\ddot{e}$ tends toward $+\infty$. On the contrary, when $EOA = A$ (no stenosis), locations 1, 2, and 3 are superimposed and $1/\lambda$ thus equals zero. The expression $1/\lambda$ is exclusively dependent upon the flow jet geometry and more precisely upon $EOA$ and $A$, so that a dimensional analysis (25) gives the following relationship:

$$\frac{\sqrt{A}}{\lambda} = \mathrm{f}\left(\frac{A}{EOA}\right) \tag{13}$$

A simple type of functions f defined on $[1\ ,\ +\infty]$ that meets the two aforementioned boundary conditions [i.e., $\mathrm{f(x)} \to +\infty$ when $\mathrm{x} \to +\infty$ and $\mathrm{f}(1) = 0$] is the following:

$$\frac{\sqrt{A}}{\lambda} = \alpha\left(\frac{A}{EOA} - 1\right)^\beta \tag{14}$$

where $\alpha$ and $\beta$ are two strictly positive constants to be determined. Integrating Equation 14 in Equation 12, $TPG_{net}$ becomes

$$TPG_{net} = \rho \frac{1}{\sqrt{A}}\frac{\partial Q}{\partial t}\alpha\left(\frac{A}{EOA} - 1\right)^\beta + \frac{1}{2}\rho Q^2 \left(\frac{1}{EOA} - \frac{1}{A}\right)^2 \tag{15}$$

It is difficult to solve $\alpha$ and $\beta$ from a purely analytical development. We therefore determined these two constants by means of *in vitro* experiments performed in a mock flow circulation model. Nine orifice plates, simulating several grades of aortic stenosis severity, were tested under numerous physiological pulsatile flow conditions. A minimization method provided $\alpha = 2\pi$ and $\beta = 1/2$ (18). From those results, the instantaneous $TPG_{net}$ is finally expressed as

$$TPG_{net} = 2\pi\rho \frac{\partial Q}{\partial t}\sqrt{\frac{1}{EOA} - \frac{1}{A}} + \frac{1}{2}\rho Q^2\left(\frac{1}{EOA} - \frac{1}{A}\right)^2 \quad (16)$$

When using the expression of the energy loss coefficient ($E_L Co$) defined as $EOA \times A / (A - EOA)$ (26), $TPG_{net}$ can be written as

$$TPG_{net} = P_{LV} - P_A = \frac{2\pi\rho}{\sqrt{E_L Co}}\frac{\partial Q}{\partial t} + \frac{\rho}{2E_L Co^2}Q^2 \quad (17)$$

Equation 17 shows that, for a given transvalvular flow rate $Q(t)$, the pressure difference between the left ventricle and the aorta, i.e., $TPG_{net}$, is dependent upon a unique valvular parameter, namely $E_L Co$. This equation was validated with bioprosthetic heart valves in the above-mentioned *in vitro* model and was shown to predict accurately the instantaneous $TPG_{net}$ measured by micromanometer-tipped Millar catheters. We invite the reader to refer to (18) for a detailed description of the complete protocol.

### 2.3. The Left Ventricular Pressure-Volume Relationship

Pressure-volume graphs are commonly used to assess the inotropic state of the left ventricle (27). When tracing LV pressure (in mmHg) as a function of LV cavity volume (in mL), a complete loop, called the pressure-volume loop (PV loop), is described. LV stroke work is the work of the left ventricle during each heart beat and is represented by the area contained within the PV loop (Figs. 3 and 11). LV stroke work has been shown to effectively characterize the outcome of patients with AS (28). If the loading conditions on the heart are pharmaceutically (e.g., by administration of phenylephrine) or mechanically (e.g., by occlusion of the inferior vena cava) modified, while myocardial contractility remains unchanged, a series of PV loops is obtained (Fig. 3). In a physiological range, the top left corners of the PV loops may be connected by a regression line (Fig. 3) whose slope is called the maximal elastance ($E_{\max}$). The intercept of this line with the abscissa volume axis is the unloaded volume ($V_0$). It should be noted that the linear approximation often leads to negative $V_0$ (29). Hence, $V_0$ has no physical or physiological meaning but should rather be considered as a virtual parameter computed by extrapolation. This linear characteristic remains, however, largely appropriate over a large physiological or pathophysiological range. In the 1970s, Suga et al. (30) defined the time-varying LV elastance as LV pressure

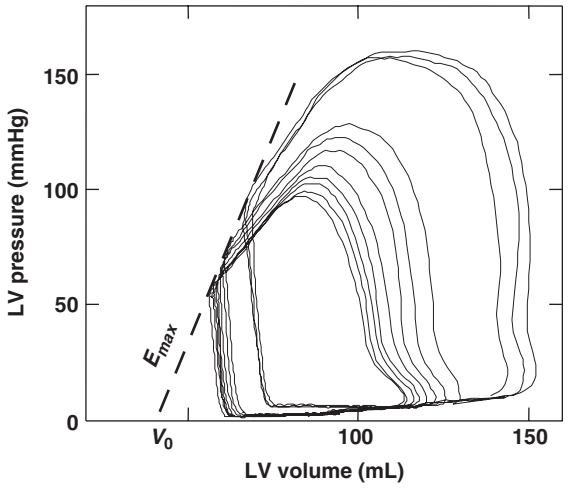


**Figure 3.** Series of left ventricular pressure-volume loops obtained in a patient with aortic stenosis. $E_{\max}$ is the maximal elastance. $V_0$ is the left ventricular unloaded volume. From Dekker et al. (36) with permission.

($P_{LV}$) divided by LV cavity volume ($V$) decremented by $V_0$:

$$E(t) = \frac{P_{LV}(t)}{V(t) - V_0} \quad (18)$$

Interestingly, it has been shown by Senzaki et al. that the elastance waveform, when normalized with respect to its amplitude ($E_{\max}$) and time to peak value ($T_{E\max}$), is somewhat similar in the normal or diseased human hearts despite the presence of differences with regard to etiology of heart disease, LV myocardial contractility and loading conditions (31). Fig. 4 depicts the normalized LV elastance ($E_N$) as a function of normalized time, as measured by Senzaki et al. in patients and normal subjects. Due to the universal property of the LV normalized elastance, LV pressure can be related to LV volume by means of only three independent LV parameters, namely $E_{\max}$, $T_{E\max}$,

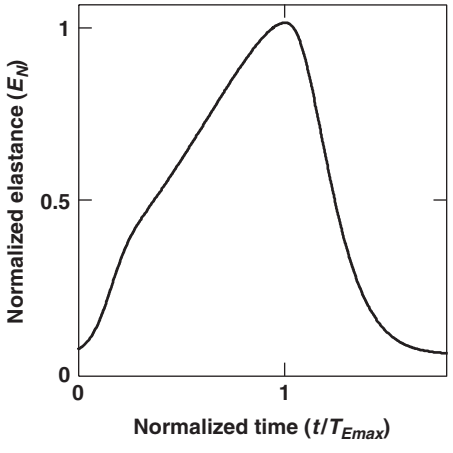


**Figure 4.** Normalized left ventricular elastance as a function of normalized time (dimensionless).

and $V_0$, as follows:

$$E_{\max}E_N\left(t/T_{E_{\max}}\right)=\frac{P_{LV}(t)}{V(t)-V_0} \tag{19}$$

### 2.4. The Three-Element Windkessel Model of the Peripheral System

The three-element windkessel (WK3) model is a lumped model that has been proven to simulate adequately the hemodynamic characteristics of the peripheral system (32,33). It includes three independent vascular parameters: the characteristic impedance of the proximal aorta ($Z_0$); the arterial compliance ($C$); and the systemic vascular resistance ($R$). The resistance $R$ reproduces the hydraulic resistance in the small arteries and arterioles, the compliance $C$ reflects the ability of the large arteries to distend with increasing inner pressure, and the characteristic impedance $Z_0$ mainly relates the transvalvular flow rate ($Q$) to the aortic pressure in the high-frequency range (highly pulsatile range). An electrical analog model of the WK3 is illustrated in Fig. 5. In this figure, $P_A$ and $P_{VE}$ represent the aortic pressure and the central venous pressure, respectively. Using complex notation, the peripheral impedance is written as

$$Z^*=Z_0+\frac{R}{1+j\omega RC} \tag{20}$$

where $\omega$ is the pulsation frequency and $j$ is the unit complex number. Then, using Ohm's law ($\Delta P=P_A-P_{VE}=Z*Q$), one obtains

$$j\omega\Delta P+\frac{\Delta P}{RC}=\frac{Z_0+R}{RC}Q+Z_0j\omega Q \tag{21}$$

what may be rewritten, in the time domain ($j\omega$ is changed to $\partial/\partial t$), as

$$\frac{\partial P_A(t)}{\partial t}+\frac{P_A(t)}{RC}=\frac{Z_0+R}{RC}Q(t)+Z_0\frac{\partial Q(t)}{\partial t}+\frac{P_{VE}}{RC} \tag{22}$$

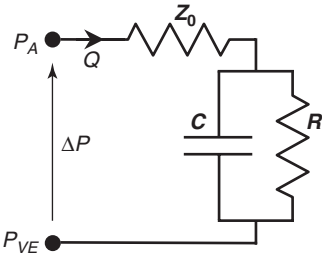


**Figure 5.** Electrical representation of the three-element windkessel model. $P_A$ = aortic pressure, $P_{VE}$ = central venous pressure, $Q$ = transvalvular flow rate. $Z_0$ = aortic characteristic impedance, $R$ = systemic vascular resistance, $C$ = arterial compliance.

We note $t_0$ the time at which LV ejection begins and $T$ the cardiac period. The analytical resolution of this linear differential equation yields the aortic pressure ($P_A$) within the time interval $[t_0;\ t_0+T]$:

$$P_A(t)=\mathrm{e}^{-(t-t_0)/RC}\left(\int_{t_0}^{t}\frac{Q^*(\tau)}{C\mathrm{e}^{-(\tau-t_0)/RC}}\mathrm{d}\tau+DP_A\right) \tag{23}$$

where $Q^*$ is related to $Q$ as follows:

$$Q^*(\tau)=\frac{Z_0+R}{R}Q(\tau)+Z_0C\frac{\partial Q(\tau)}{\partial\tau}+\frac{P_{VE}}{R} \tag{24}$$

and where the diastolic blood pressure ($DP_A$) can be determined using the periodic property of $P_A$ and is given by

$$DP_A=\int_{t_0}^{t_0+T}\frac{Q^*(t)\mathrm{e}^{(t-t_0)/RC}}{C\mathrm{e}^{T/RC}-C}\mathrm{d}t \tag{25}$$

For a given central venous pressure, the WK3 representation described by Equations 23–25 thus relates aortic pressure to transvalvular flow rate using only three vascular parameters ($Z_0$, $R$, and $C$).

### 2.5. The $V^3$ (Ventricular-Valvular-Vascular) Model

**2.5.1. Derivation of the $V^3$ Model.** The ventricular-valvular-vascular $V^3$ model results from the coupling of the abovementioned LV time-varying elastance, $TPG_{net}$ equation and WK3 model (Fig. 6). The sum $\partial$(Equation 17)/$\partial t$ + (Equation 17)/($RC$) yields

$$\begin{aligned}&\left(\frac{\partial P_{LV}}{\partial t}+\frac{P_{LV}}{RC}\right)-\left(\frac{\partial P_A}{\partial t}+\frac{P_A}{RC}\right)\\&=\frac{2\pi\rho}{\sqrt{E_LCo}}\left(\frac{\partial^2Q}{\partial t^2}+\frac{1}{RC}\frac{\partial Q}{\partial t}\right)+\frac{\rho}{2}\frac{Q}{E_LCo^2}\left(2\frac{\partial Q}{\partial t}+\frac{Q}{RC}\right)\end{aligned} \tag{26}$$

The expression ($\partial P_A/\partial t+P_A/RC$) in Equation 26 is expressed as a function of $Q$ using Equation 22, and $P_{LV}$ is replaced using Equation 19. Throughout ejection, transvalvular flow rate can be written as: $Q(t)=-\partial V(t)/\partial t$. Therefore, Equation 26 becomes

$$\begin{aligned}\frac{2\pi\rho}{\sqrt{E_LCo}}\frac{\partial^3V(t)}{\partial t^3}&=a_3(t)\frac{\partial^2V(t)}{\partial t^2}+a_2(t)\frac{\partial V(t)}{\partial t}\\&\quad+a_1(t)V(t)+a_0(t)\end{aligned}$$

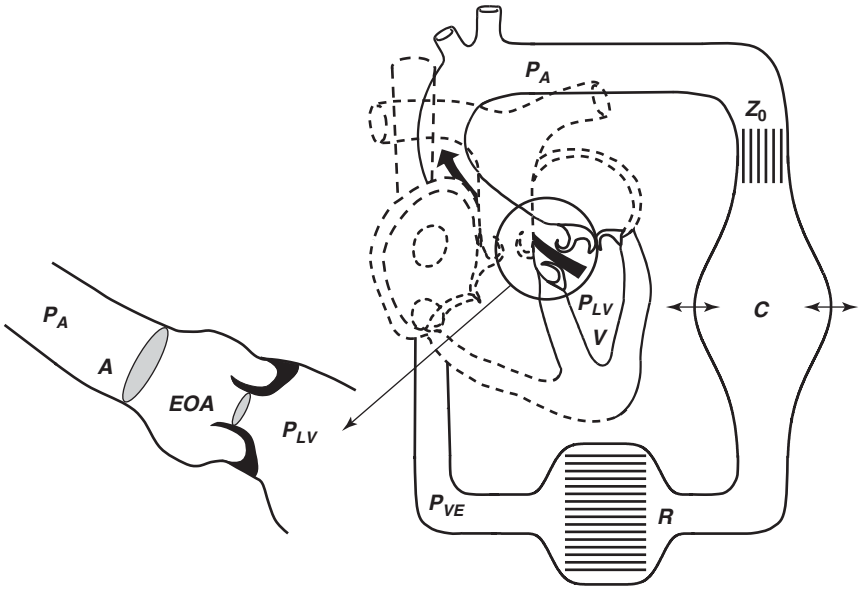


**Figure 6.** Schematic representation of the $V^3$ model. $V$ = left ventricular cavity volume, $P_{LV}$ = left ventricular pressure, $P_A$ = aortic pressure. See also legends of Figs. 2 and 5. From Garcia et al. (19) with permission.

where

$$\begin{aligned} a_0(t) &= V_0 \frac{E_{\max}}{T_{E_{\max}}} \frac{\partial E_N(\hat{t})}{\partial \hat{t}} + V_0 E_{\max} \frac{E_N(\hat{t})}{RC} + \frac{P_{VE}}{RC} \\ a_1(t) &= -\frac{E_{\max}}{T_{E_{\max}}} \frac{\partial E_N(\hat{t})}{\partial \hat{t}} - E_{\max} \frac{E_N(\hat{t})}{RC} \\ a_2(t) &= \frac{\rho}{2RCE_L Co^2} \frac{\partial V(t)}{\partial t} - \frac{Z_0 + R}{RC} - E_{\max} E_N(\hat{t}) \\ a_3(t) &= \frac{\rho}{E_L Co^2} \frac{\partial V(t)}{\partial t} - \frac{2\pi\rho}{RC\sqrt{E_L Co}} - Z_0 \end{aligned} \tag{27}$$

where $\hat{t}$ is the normalized time ($t/T_{Emax}$). At the onset of the ejection (at $t = t_0$), $LV$ volume $V$ is equal to the LV end-diastolic volume ($V(t_0) = LVEDV$) and $Q(t_0) = 0$. LV ejection begins when LV pressure reaches aortic pressure and $TPG_{net}$ thus equals zero. According to Equation 17, $\partial Q/\partial t$ is therefore also equal to 0 at the ejection onset. Because $Q(t) = -\partial V(t)/\partial t$ during LV ejection, the initial conditions are therefore

$$V(t_0) = LVEDV;\ \frac{\partial V}{\partial t}(t_0) = 0;\ \frac{\partial^2 V}{\partial t^2}(t_0) = 0 \tag{28}$$

The 3rd-order nonlinear differential equation 27, with the corresponding initial conditions (Equation 28), describes thoroughly the LV volume during ejection under the conditions that the ventricular, valvular, and vascular properties are given. Table 1 summarizes the independent input parameters necessary for solving the $V^3$ model. The mathematical $V^3$ model has been validated in patients during surgery, before and after aortic valve replacement, as described in details in (19).

**2.5.2. Numerical Computation.** Time reference ($t = 0$) is fixed at the onset of the isovolumic LV contraction. An arbitrary diastolic pressure ($DP_A$) is chosen and $t_0$ (onset of ejection) is then determined from Equation 19 such that it satisfies the following condition: $E_{\max} E_N(t_0/T_{E\max}) = DP_A/(LVEDV - V_0)$. LV cavity volume during ejection, $V(t)$, is then calculated from Equation 27 using an explicit Runge–Kutta method starting from $t_0$ until $\partial V(t)/\partial t$ reaches zero. Transvalvular flow rate during LV ejection is $Q(t) = -\partial V(t)/\partial t$ and is further assumed to be zero throughout the rest of the cardiac cycle (no aortic regurgitation). Aortic pressure is then deduced from Equations 23–25 and a second $DP_A$ is therefore obtained. If the difference between the two $DP_A$ exceeds a given relative error, a new iteration is performed using the latest $DP_A$ value until the desired precision is reached. Knowing $V(t)$, LV pressure during isovolumic contraction, ejection, and isovolumic relaxation is finally calculated by means of Equation 19 and is linearly extrapolated during the LV filling. LV volume during LV filling is extrapolated using a 2nd-order polynomial so that its temporal derivative is zero at the end of diastole. A detailed Matlab program for the resolution of the $V^3$ model is available online in (34). Figure 7 shows normal physiological waveforms simulated with the $V^3$ model (normotensive condition, normal aortic valve, and normal cardiac conditions). It should be noted that the $V^3$ model in the present form may exclusively simulate LV volume and pressure for the periods of ejection and isovolumic contraction and relaxation. Their waveforms during LV filling are thereby extrapolated. Thus, the $V^3$ model as presented here cannot be used to analyze LV diastolic dysfunction.

## 3. APPLICATIONS

The $V^3$ model provides a potentially useful tool for simulating the effects of AS on pressure and transvalvular flow waveforms with different grades of AS severity. To date, no explicit theoretical model has been shown to reflect accurately the cardiovascular hemodynamics in presence of AS (19). As for the $V^3$ model, it may explicitly and correctly

**Table 1. List of the Cardiovascular Input Parameters Required for the Resolution of the V3 Model [Values in the right column are typical physiological values used for the simulations with a heart rate of 70 beats per minute. Emax (mmHg/mL), R (mmHg.s/mL) and C (mL/mmHg) were adjusted according to the desired hemodynamic conditions as explained in the text (see also Table 3). EOA was varied from 4 cm2 (no aortic stenosis) down to 0.5 cm2 (severe stenosis).]**

| | | |
|---|---|---|
| **Ventricular parameters** | | |
| Left-ventricular end-diastolic volume | LVEDV | 150 mL |
| Unloaded volume | $V_0$ | 15 mL |
| Maximal elastance | $E_{max}$ | Adjusted for stroke volume (70 mL) |
| Time to maximal elastance | $T_{Emax}$ | 0.33 s |
| **Vascular parameters** | | |
| Aortic characteristic impedance | $Z_0$ | 0.07 mmHg s/mL |
| Systemic vascular resistance | $R$ | Adjusted for blood pressure level |
| Total arterial compliance | $C$ | Adjusted for blood pressure level |
| Central venous pressure | $P_{VE}$ | 5 mmHg |
| **Valvular parameters** | | |
| Effective orifice area | $EOA$ | From 4 down to 0.5 cm2 |
| Aortic cross-sectional area | $A_A$ | 5 $cm^2$ |

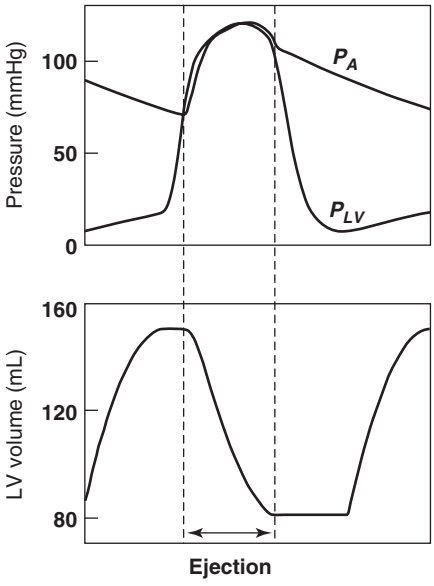


**Figure 7.** Top—left ventricular ($P_{LV}$) and aortic pressure ($P_A$) waveforms simulated with the $V^3$ model under normal conditions. Bottom—corresponding simulated left ventricular cavity volume. Time scale covers more than one cardiac cycle.

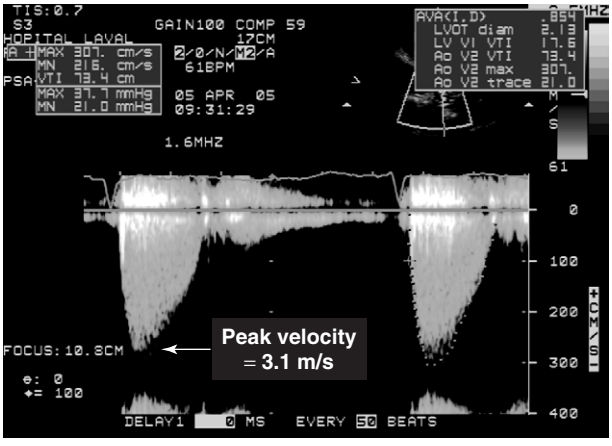


**Figure 8.** Continuous-wave Doppler recording of an aortic stenosis jet in a patient with severe aortic stenosis ($EOA = 0.85\,cm^2$).

describe some cardiovascular features if only a few cardiovascular parameters are known, and as importantly, its validity has been tested in patients with AS. In clinical practice, AS is graded as mild if $EOA > 1.5$ $cm^2$, moderate if $EOA > 1.0$ and $\leq 1.5\,cm^2$, or severe if $EOA \leq 1.0\,cm^2$ (Table 2). When stenosis is severe and cardiac output is normal, the mean $TPG_{net}$ is generally $> 50$ mmHg (1 mmHg $\approx$ 133 Pa) (35). Because it is cost-effective, completely non-invasive, and rapid, echocardiography is presently the most commonly applied modality in clinical cardiology for establishing the diagnosis of aortic stenosis. Echocardiography allows one to display high-quality images of the heart as well as the transvalvular blood velocities (Fig. 8). Doppler echocardiography is mainly used to determine $EOA$ by means of the continuity equation (equation of mass conservation). The peak velocity across the valve (at location 2, Fig. 2) measured by Doppler echocardiography has also been shown to be predictive of symptom onset in AS patients (Fig. 8) (1). When the clinical and echocardiographic data yield conflicting diagnoses or when the echocardiographic data are unconvincing, invasive measurements by cardiac catheterization are needed and max or mean $TPG_{net}$ are measured (Fig. 9), among other parameters. When severity of AS becomes significant, pressure loss due to the aperture narrowing of the valve induces an increase in LV cavity pressure and LV stroke work. If concomitant HPT is present, effects of AS on LV function are worsened due to the further vascular overload. The following paragraphs will show how AS may affect LV pressure and more specifically LV stroke work, by using the numerical $V^3$ model. The additional effect of concomitant HPT will then be described.

### 3.1. Simulations of Flow and Pressure Waveforms with Aortic Stenosis

The ejection fraction is defined as the amount of blood ejected divided by the amount of blood contained in the left

**Table 2. Classification of Hypertension and Aortic Stenosis Severity According to the European Society of Hypertension (44) and to the American College of Cardiologỹ/ American Heart Association (35) (Systolic and diastolic pressures are in mmHg. *EOA*˜ = effective orifice area.)**

| | Hypertension | | Aortic Stenosis |
|---|---|---|---|
| | Systolic | Diastolic | *EOA* |
| Normal | 120–129 | 80–84 | $\geq 3\,cm^2$ |
| High normal | 130–139 | 85–89 | |
| Mild | 140–159 | 90–99 | $> 1.5\,cm^2$ |
| Moderate | 160–179 | 100–109 | $1.0–1.5\,cm^2$ |
| Severe | $\geq 180$ | $\geq 110$ | $\leq 1.0\,cm^2$ |

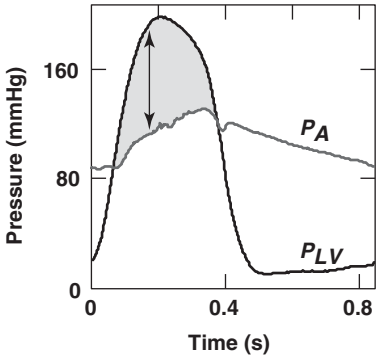


**Figure 9.** Typical left ventricular ($P_{LV}$) and aortic pressure ($P_A$) waveforms in a patient with severe aortic stenosis. The arrow represents the peak $TPG_{net}$ (net transvalvular pressure gradient). During a clinical examination, mean $TPG_{net}$ is calculated as the gray area divided by ejection time.

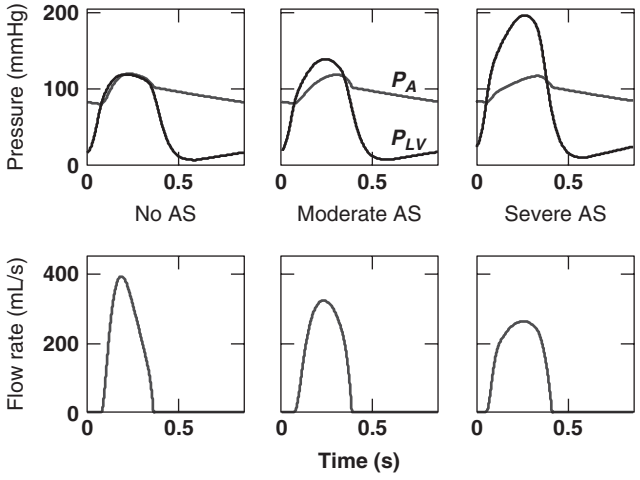


**Figure 10.** Pressure and transvalvular flow waveforms simulated with the $V^3$ model. Note that simulated pressure waveforms with severe aortic stenosis are similar to those measured in patient (Fig. 9).

ventricle at end of diastole. In absence of serious LV dysfunction, ejection fraction is usually normal (50–60 %) in patients with AS (7). For a normal average stroke volume of 70 mL, *LVEDV* is therefore maintained at ~150 mL. In addition, typical values are assumed for $V_0$ (15 mL), $T_{\mathrm{Emax}}$ (0.33 s), $A$ ($5\,cm^2$), $Z_0$ (0.07 mmHg.s/mL) and $P_{VE}$ (5 mmHg) to achieve the simulations (19,36). The heart rate was fixed at 70 beats per minute and maximal elastance ($E_{\max}$) was adjusted so that stroke volume equals 70 mL (normal outflow condition). For example, the respective calculated values for $E_{\max}$ without AS and with very severe AS ($EOA = 0.5\ cm^2$) were 1.63 and 2.35 mmHg/mL. Total vascular resistance ($R$) and arterial compliance ($C$) were also adjusted to obtain normotensive conditions (systolic/diastolic pressures = 120/80 mmHg): their respective values were 1.07 mmHg.s/mL and 2.05 mL/mmHg. Table 1 summarizes the chosen values for the input cardiovascular parameters. Figure 10 illustrates three simulations achieved with the $V^3$model: (1) no AS ($EOA = 4\,cm^2$); (2) moderate AS ($EOA = 1\,cm^2$); and (3) severe AS ($EOA = 0.5\,cm^2$). This figure shows that simulated LV and aortic pressure waveforms are very similar to those observed in patients (see Fig. 9 for comparison). Whereas LV peak pressure has a normal value (120 mmHg) without AS, it may be as high as 200 mmHg with very severe AS, even under normotensive conditions.

It has been reported that ejection time lengthens (37,38) and that peak transvalvular flow rate occurs later in ejection with increasing AS severity (39,40). The simulated instantaneous transvalvular flow rates are very consistent with these observations as shown in Fig. 10. Figure 11 illustrates the PV loops corresponding to the conditions of Fig. 10. Stroke work ($SW = P_{LV}dV$, represented by the inner area of PV loops) increases significantly when *EOA* decreases, i.e., when severity of AS increases. Figure 12 shows more accurately how LV stroke work varies with AS severity. It can be observed that LV stroke work remains relatively stable around the value of 1 J when $EOA > 1\,cm^2$, which means that AS does not greatly affect the LV pump when graded as mild or even moderate. But when AS is severe ($EOA < 1\,cm^2$), a small decrease in *EOA* induces a drastic increase in LV stroke work, and it is precisely in this range that patients with AS generally develop symptoms.

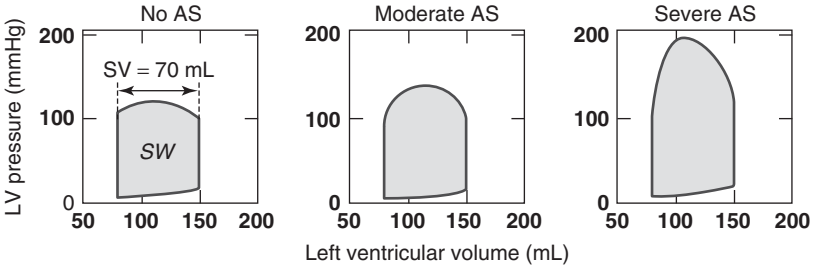


**Figure 11.** Simulated left ventricular pressure-volume loops for the hemodynamic conditions illustrated in Fig. 10. Left ventricular stroke work (SW) is represented by the inner area. SV is stroke

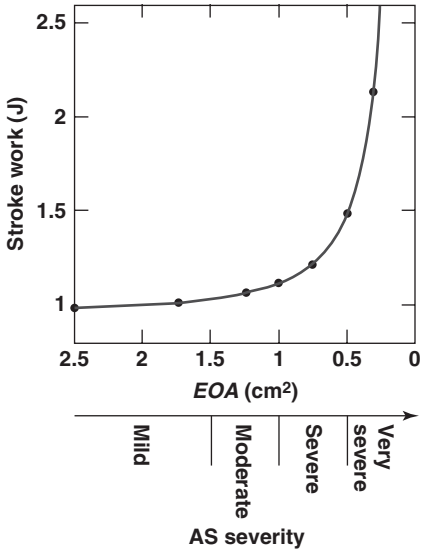


**Figure 12.** Left ventricular stroke work as a function of aortic stenosis severity. One dot characterizes one simulation performed with the $V^3$ model.

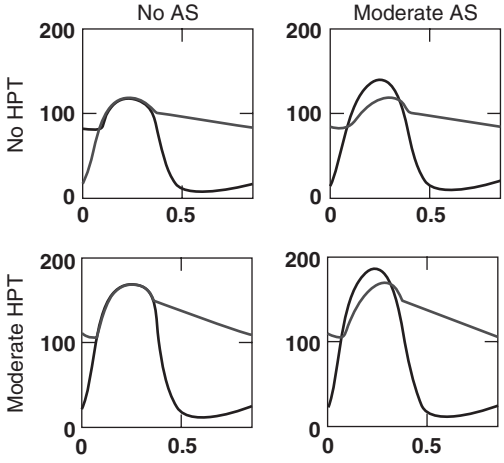


**Figure 13.** Simulated left ventricular ($P_{LV}$) and aortic ($P_A$) pressures in normal aortic valve (no AS) and moderate aortic stenosis (AS) with and without moderate hypertension (HPT). Pressures are in mmHg, time is in s.

### 3.2. Simulations in the Presence of Aortic Stenosis and Coexistent Systemic Hypertension

Left ventricular pressure overload caused by AS or systemic arterial HPT generally results in LV concentric hypertrophy, which has been shown to be a strong independent risk factor for morbidity and mortality (41,42). Systemic hypertension (HPT) has a prevalence of 30–40 % in patients with AS (4,43). The resulting vascular overload in such patients adds further to the valvular overload, which increases the LV afterload and affects LV function and patient outcome. The $V^3$ model may help to quantify the respective impacts of AS and HPT on LV function. For this purpose, we simulated the combined effect of AS and HPT on the LV stroke work. Aortic stenosis severity was varied from mild to severe ($EOA = 1.75$ to $0.5\,cm^2$), and for each degree of AS severity, blood pressure level was progressively increased from normotensive conditions to severe HPT (systolic/diastolic pressures = 120/80 to 190/115 mmHg). For each degree of HPT, systemic vascular resistance ($R$) and arterial compliance ($C$) were adjusted to obtain the desired systolic and diastolic aortic pressures (Table 3). Systolic and diastolic aortic pressures were chosen according to the classification of blood pressure levels published by the European Hypertension Society (44) (Table 2). The values found for $R$ and $C$ were comparable to those measured in hypertensive patients (45,46).

As mentioned previously, $E_{max}$ was adjusted for each simulation so that stroke volume was equal to 70 mL. The chosen values of the other input cardiovascular parameters are listed in Table 1. Figure 13 illustrates four simulations obtained with a normal valve and a moderate aortic stenosis ($EOA = 1\,cm^2$) with and without moderate hypertension (170/105 mmHg). The peak LV pressure is largely increased when hypertension coexists with AS (no AS = 120, moderate AS = 139, moderate HPT = 169, moderate AS + HPT = 185 mmHg). It should also be noted that moderate AS has a small impact on LV stroke work in comparison with moderate HPT (no AS = 1.00, moderate AS = 1.11, moderate HPT = 1.37, moderate AS + HPT = 1.47 J). The following valvular parameters: peak $TPG_{net}$, mean $TPG_{net}$, and peak jet velocity (Table 4) were very consistent with those of patients reported in the literature (1,22). As an example, mean $TPG_{net}$ and peak jet velocity with an $EOA$ of $0.5\,cm^2$ were found to be 55 mmHg and 5.3 m/s, respectively, which represent typical values for patients with severe AS (1). As expected, because cardiac flow conditions were fixed, these parameters were only dependent upon AS severity and were not influenced by the degree of HPT (Table 4). The theoretical influence of AS/HPT on LV stroke work is represented on Fig. 14. This graph shows that LV stroke work is shifted upward from one blood pressure level to the following, independently of the AS grade AS. Thus, HPT has a quasi-linear effect on LV work. By contrast, an increase in AS severity from mild to moderate ($EOA > 1\,cm^2$) has a very small impact on LV

**Table 3. Values of Total Peripheral Resistance ($R$) and Arterial Compliance ($C$) Utilized for Simulating the Different Blood Pressure Levels in This Study**

| Blood Pressure Level | Arterial Pressure (mmHg) | | R (mmHg.s/mL) | C (mL/mmHg) |
|---|---|---|---|---|
| | Systolic | Diastolic | | |
| Normal | 120 | 80 | 1.07 | 2.05 |
| High normal | 135 | 87 | 1.21 | 1.47 |
| Mild | 150 | 95 | 1.35 | 1.23 |
| Moderate | 170 | 105 | 1.53 | 0.98 |
| Severe | 190 | 115 | 1.71 | 0.83 |

**Table 4. Hemodynamic Valvular Parameters Obtained with the $V^3$ Model for Given Degrees of Aortic Stenosis Severity Under Normal Flow Conditions and Different Levels of Arterial Blood Pressure (stroke volume = 70 mL, heart rate = 70 bpm) (Values are represented as mean ± standard deviation.)**

| Aortic Stenosis | | Mean $TPG_{net}$ (mmHg) | Peak $TPG_{net}$ (mmHg) | Peak Velocity (m/s) |
|---|---|---|---|---|
| | $EOA$ | | | |
| No AS | $4\,cm^2$ | $0.8 \pm 0.7$ | $11.7 \pm 2.0$ | $1.1 \pm 0.03$ |
| Mild | $1.75\,cm^2$ | $4.5 \pm 0.5$ | $18.1 \pm 2.3$ | $2.1 \pm 0.02$ |
| Moderate | $1.25\,cm^2$ | $9.7 \pm 0.7$ | $22.0 \pm 2.3$ | $2.7 \pm 0.01$ |
| Moderate to severe | $1.0\,cm^2$ | $15.2 \pm 0.8$ | $27.2 \pm 1.0$ | $3.2 \pm 0.01$ |
| Severe | $0.75\,cm^2$ | $26.4 \pm 0.6$ | $42.8 \pm 0.7$ | $3.9 \pm 0.01$ |
| Very severe | $0.5\,cm^2$ | $55.4 \pm 1.3$ | $84.7 \pm 1.1$ | $5.3 \pm 0.03$ |

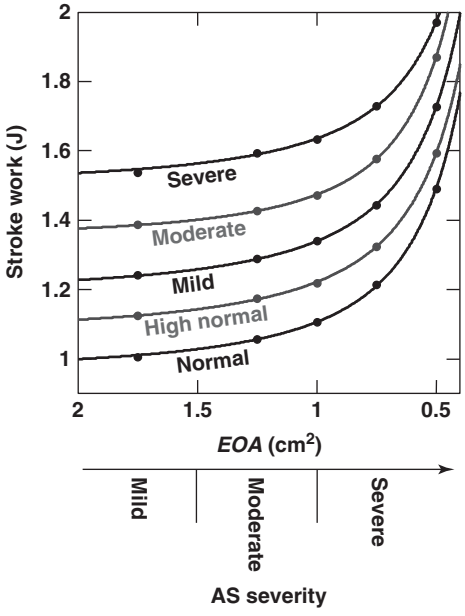


**Figure 14.** Left ventricular stroke work as a function of aortic stenosis severity for normal arterial pressure and different grades of hypertension. One dot characterizes one simulation performed with the $V^3$ model.

stroke work. The latter, however, increases noticeably when AS becomes severe ($EOA < 1 cm^2$).

### 3.3. Potential Clinical Implications

According to current guidelines, the decision to replace a stenotic valve is mainly based on $EOA$ and presence of symptoms (35). Unfortunately, there are often discrepancies between the AS severity and the symptomatic status. Some patients are indeed symptomatic although they have only a moderate AS, whereas others remain asymptomatic despite the presence of severe AS. Our simulations may in part explain these discrepancies. According to our numerical results, a patient having moderate AS with coexistent moderate HPT may have higher LV afterload than a normotensive patient with severe AS. Accordingly, HPT is a well-established cardiovascular risk factor. Its impact on the clinical outcome of patients with AS, however, is still unknown (47), but it has been recently reported that in hypertensive symptomatic AS patients, symptoms of AS develop at a relative earlier stage of the disease, with larger $EOA$ (4). This is very likely due to the additional LV afterload induced by HPT itself, because our simulations tended to show that even mild HPT may greatly influence LV stroke work and therefore LV function in AS patients. Thus, antihypertensive medication should be initiated soon after aortic valve replacement in patients with coexistent HPT. As an example, Fig. 15 illustrates a hypothetical case of a patient with moderate HPT (systolic/diastolic pressures = 170/105 mmHg), severe AS ($EOA = 0.6\,cm^2$), and normal output flow conditions (stroke volume = 70 mL, heart rate = 70 bpm), whose left ventricle develops a stroke work of 1.75 J. In such a patient, aortic valve replacement alone would reduce LV stroke work to 1.4 J. This is identical to the work done by the left ventricle in presence of severe AS (with an $EOA$ of $0.6\,cm^2$) under normotensive conditions. Thus, this patient would not fully benefit from aortic valve replacement if no antihypertensive medication was prescribed, since LV stroke work would remain abnormally high. This could explain why short-term clinical results vary considerably from one patient to another after aortic valve replace-

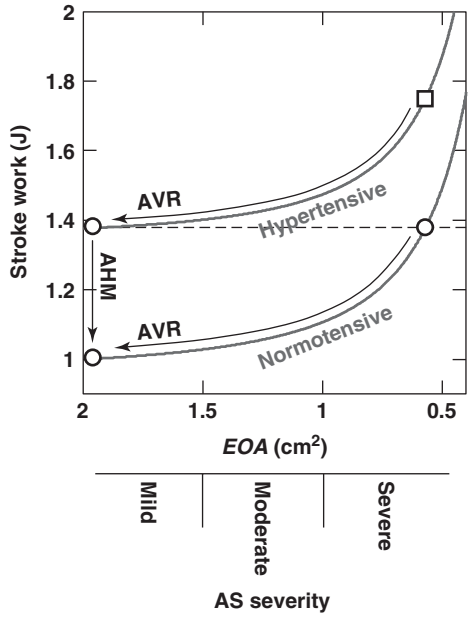


**Figure 15.** Respective outcome of aortic valve replacement (AVR) and antihypertensive medication (AHM) in a patient (represented by a square) with severe aortic stenosis and moderate systemic hypertension.

ment. This surgery removes the valvular component of the LV overload but not its vascular component related to HPT. Hence, patients with AS and concomitant HPT may have only minimal LV functional outcome if aortic valve replacement alone is carried out. The influence of HPT on the development of LV overload and symptoms in patients with AS is often underestimated in the clinical practice, while the $V^3$ model shows that HPT, even at mild degree, is an important determinant of LV stroke work in patients with AS.

## 4. FUTURE INVESTIGATIONS

The $V^3$ model has been proved to predict accurately LV pressure, aortic pressure, and LV volume waveforms in patients with AS (19). Contrary to previously published mathematical models of the cardiovascular circulation, the $V^3$ model contains a realistic representation of the transvalvular pressure-flow relationship. Because the cardiovascular input parameters are all measurable *in vivo*, it may also enlighten clinical inquiries with regard to the effects of some cardiovascular diseases on the LV function. In addition, future updates could be made to extend its clinical applications. As an example, combining the $V^3$ model with the lumped representation of left coronary circulation developed by Judd and Mates (48) could allow the examination of the impact of AS and HPT on coronary blood flow, and would help to clarify the occurrence of LV failure in patients with AS and/or HPT. Indeed, the left coronary circulation is essentially governed by LV pressure and by the left coronary inlet pressure (49). Also, in the current version of the $V^3$ model, *EOA* is supposed constant throughout ejection. Whereas this hypothesis is adequate in normal and mildly or moderately calcified aortic valves, it has been reported that *EOA* may vary notably during ejection in patients with severe AS (39,50). Time-dependence of *EOA* may significantly influence $TPG_{net}$ and LV pressure waveforms and consequently LV stroke work. The influence of time-varying *EOA* on LV stroke work could be studied by writing *EOA* as a function of transvalvular flow. This could be performed for example by means of a simple spring-damper representation of the valve aperture or by using a Lagrangian dynamic leaflet model as that proposed by Fenlon and David (51). Despite its relative simplicity, the $V^3$model may therefore allow the investigation of complex cardiovascular interactions. In conclusion, mathematical cardiovascular models, such as the $V^3$ model, may answer important clinical questions. It is, however, essential to experimentally validate the model per se and its findings before any clinical application.

### Acknowledgments

The authors gratefully thank Dr. Lysanne Goyer and Dr. Lyes Kadem, from the Institut de Recherches Cliniques de Montréal, for having carefully reviewed this chapter.

## BIBLIOGRAPHY

1. D. M. Shavelle and C. M. Otto, Aortic stenosis. In: Crawford MH, Dimarco JP, ed., Cardiology. London: Mosby, 2000: 9.1–9.9.
2. P. Tornos, [New aspects in aortic valve disease]. *Rev. Esp. Cardiol*. 2001; **54**(Suppl 1):17–21.
3. R. A. Nishimura, Cardiology patient pages. *Aortic valve disease. Circulation* 2002; **106**(7):770–772.
4. F. Antonini-Canterin, G. Huang, E. Cervesato, P. Faggiano, D. Pavan, R. Piazza, and G. L. Nicolosi, Symptomatic aortic stenosis: Does systemic hypertension play an additional role? *Hypertension* 2003; **41**(6):1268–1272.
5. M. Briand, J. G. Dumesnil, L. Kadem, A. G. Tongue, R. Rieu, D. Garcia, and P. Pibarot, Reduced systemic arterial compliance impacts significantly on LV afterload and function in aortic stenosis: Implications for diagnosis and treatment. *J. Am. Coll. Cardiol*. 2005; **46**(2):291–298.
6. M. E. Safar, B. I. Levy, and H. Struijker-Boudier, Current perspectives on arterial stiffness and pulse pressure in hypertension and cardiovascular diseases. *Circulation* 2003; **107**(22):2864–2869.
7. K. E. Berkina and S. G. Ball, Essential hypertension: The heart and hypertension. *Heart* 2001; **86**(4):467–475.
8. W. Grossman, D. Jones, and L. P. McLaurin, Wall stress and patterns of hypertrophy in the human left ventricle. *J. Clin. Invest.* 1975; **56**(1):56–64.
9. D. H. Fitchett, LV-arterial coupling: interactive model to predict effect of wave reflections on LV energetics. *Am. J. Physiol*. 1991; **261**(4 Pt 2):H1026–H1033.
10. R. R. Ha, J. Qian, D. L. Ware, J. B. Zwischenberger, A. Bidani, and J. W. Clark, An integrative cardiovascular model of the standing and reclining sheep. *Cardiovasc. Eng*. 2005; **5**(2):53–75.
11. T. Korakianitis and Y. Shi, Numerical simulation of cardiovascular dynamics with healthy and diseased heart valves. *J. Biomech*. 2005; doi:10.1016/j.jbiomech.2005.06.016.

12. J. K. Li, J. Y. Zhu, and M. Nanna, Computer modeling of the effects of aortic valve stenosis and arterial system afterload on left ventricular hypertrophy. *Comput. Biol. Med.* 1997; **27**(6):477–485.
13. P. Segers, N. Stergiopulos, and N. Westerhof, Quantification of the contribution of cardiac and arterial remodeling to hypertension. *Hypertension* 2000; **36**(5):760–765.
14. B. W. Smith, J. G. Chase, R. I. Nokes, G. M. Shaw, and G. Wake, Minimal haemodynamic system model including ventricular interaction and valve dynamics. *Med. Eng. Phys.* 2004; **26**(2):131–139.
15. N. Stergiopulos, J. J. Meister, and N. Westerhof, Determinants of stroke volume and systolic and diastolic aortic pressure. *Am. J. Physiol.* 1996; **270**(6 Pt 2):H2050–H2059.
16. M. Ursino, Interaction between carotid baroregulation and the pulsating heart: A mathematical model. *Am. J. Physiol.* 1998; **275**(5 Pt 2):H1733–H1747.
17. M. Zacek and E. Krause, Numerical simulation of the blood flow in the human cardiovascular system. *J. Biomech.* 1996; **29**(1):13–20.
18. D. Garcia, P. Pibarot, and L. G. Durand, Analytical modeling of the instantaneous pressure gradient across the aortic valve. *J. Biomech.* 2005; **38**(6):1303–1311.
19. D. Garcia, P. J. Barenbrug, P. Pibarot, A. L. Dekker, F. H. van der Veen, J. G. Maessen, J. G. Dumesnil, and L. G. Durand, A ventricular-vascular coupling model in presence of aortic stenosis. *Am. J. Physiol. Heart Circ. Physiol.* 2005; **288**(4):H1874–H1884.
20. A. J. Ward-Smith, Internal fluid flow. The fluid dynamics of flow in pipes and ducts. Oxford: Clarendon Press, 1980.
21. D. S. Miller, Internal flow systems. second ed. Bedford: BHR, 1996.
22. H. Baumgartner, T. Stefenelli, J. Niederberger, H. Schima, and G. Maurer, "Overestimation" of catheter gradients by Doppler ultrasound in patients with aortic stenosis: a predictable manifestation of pressure recovery. *J. Am. Coll Cardiol.* 1999; **33**(6):1655–1661.
23. J. D. Thomas, and Z. B. Popovic, Intraventricular pressure differences: A new window into cardiac function. *Circulation* 2005; **112**(12):1684–1686.
24. B. R. Munson, D. F. Young, and T. H. Okiishi, Viscous flow in pipes. Fundamentals of fluid mechanics. Second edition. New York: John Wiley & Sons, Inc., 1994: 455–547.
25. A. A. Sonin, A generalization of the Pi-theorem and dimensional analysis. *Proc. Natl. Acad. Sci. U S A.* 2004; **101**(23):8525–8526.
26. D. Garcia, P. Pibarot, J. G. Dumesnil, F. Sakr, and L. G. Durand, Assessment of aortic valve stenosis severity: A new index based on the energy loss concept. *Circulation* 2000; **101**(7):765–771.
27. D. Burkhoff, I. Mirsky, and H. Suga, Assessment of systolic and diastolic ventricular properties via pressure-volume analysis: A guide for clinical, translational, and basic researchers. *Am. J. Physiol. Heart Circ. Physiol.* 2005; **289**:H501–H512.
28. J. Bermejo, R. Odreman, J. Feijoo, M. M. Moreno, P. Gomez-Moreno, and M. A. Garcia-Fernandez, Clinical efficacy of Doppler-echocardiographic indices of aortic valve stenosis: A comparative test-based analysis of outcome. *J. Am. Coll. Cardiol.* 2003; **41**(1):142–151.
29. D. A. Kass, and W. L. Maughan, From 'Emax' to pressure-volume relations: A broader view. *Circulation* 1988; **77**(6):1203–1212.
30. H. Suga, K. Sagawa, and A. A. Shoukas, Load independence of the instantaneous pressure-volume ratio of the canine left ventricle and effects of epinephrine and heart rate on the ratio. *Circ. Res.* 1973; **32**(3):314–322.
31. H. Senzaki, C. H. Chen, and D. A. Kass, Single-beat estimation of end-systolic pressure-volume relation in humans. A new method with the potential for noninvasive application. *Circulation* 1996; **94**(10):2497–2506.
32. R. Fogliardi, M. Di Donfrancesco, and R. Burattini, Comparison of linear and nonlinear formulations of the three-element windkessel model. *Am. J. Physiol.* 1996; **271**(6 Pt 2):H2661–H2668.
33. N. Westerhof, G. Elzinga, and P. Sipkema, An artificial arterial system for pumping hearts. *J. Appl. Physiol.* 1971; **31**(5):776–781.
34. D. Garcia, Personal home page. http://garciadam.free.fr. 2006.
35. R. O. Bonow, B. Carabello, A. C. De Leon, L. H. Edmunds, Jr., B. J. Fedderly, M. D. Freed, W. H. Gaasch, C. R. McKay, R. A. Nishimura, P. T. O'Gara, R. A. O'Rourke, S. H. Rahimtoola, J. L. Ritchie, M. D. Cheitlin, K. A. Eagle, T. J. Gardner, A. Garson, Jr., R. J. Gibbons, R. O. Russell, T. J. Ryan, and S. C. Smith, Jr. Guidelines for the management of patients with valvular heart disease: executive summary. A report of the American College of Cardiology/American Heart Association Task Force on Practice Guidelines (Committee on Management of Patients with Valvular Heart Disease). *Circulation* 1998; **98**(18):1949–1984.
36. A. L. Dekker, P. J. Barenbrug, F. H. van der Veen, P. Roekaerts, B. Mochtar, and J. G. Maessen, Pressure-volume loops in patients with aortic stenosis. *J. Heart Valve Dis.* 2003; **12**(3):325–332.
37. R. J. Bache, Y. Wang, and J. C. Greenfield, Jr. Left ventricular ejection time in valvular aortic stenosis. *Circulation* 1973; **47**(3):527–533.
38. P. Kligfield, P. Okin, R. B. Devereux, H. Goldberg, and J. S. Borer, Duration of ejection in aortic stenosis: effect of stroke volume and pressure gradient. *J. Am. Coll. Cardiol.* 1984; **3**(1):157–161.
39. L. M. Beauchesne, R. deKemp, K. L. Chan, and I. G. Burwash, Temporal variations in effective orifice area during ejection in patients with valvular aortic stenosis. *J. Am. Soc. Echocardiogr.* 2003; **16**(9):958–964.
40. J. Chambers, R. Rajani, M. Hankins, and R. Cook, The peak to mean pressure decrease ratio: a new method of assessing aortic stenosis. *J. Am. Soc. Echocardiogr.* 2005; **18**(6):674–678.
41. K. Yamamoto, Q. N. Dang, Y. Maeda, H. Huang, R. A. Kelly, and R. T. Lee, Regulation of cardiomyocyte mechanotransduction by the cardiac cycle. *Circulation* 2001; **103**(10):1459–1464.
42. B. H. Lorell and B. A. Carabello, Left ventricular hypertrophy: Pathogenesis, detection, and prognosis. *Circulation* 2000; **102**(4):470–479.
43. G. E. Pate, Association between aortic stenosis and hypertension. *J. Heart Valve Dis.* 2002; **11**(5):612–614.
44. Guidelines committee. 2003 European Society of Hypertension-European Society of Cardiology guidelines for the management of arterial hypertension. *J. Hypertens.* 2003; **21**(6):1011–1053.
45. D. Chemla, I. Antony, Y. Lecarpentier, and A. Nitenberg, Contribution of systemic vascular resistance and total arterial compliance to effective arterial elastance in humans. *Am. J. Physiol. Heart Circ. Physiol.* 2003; **285**(2):H614–H620.

46. D. Chemla, J. L. Hebert, C. Coirault, K. Zamani, I. Suard, P. Colin, and Y. Lecarpentier, Total arterial compliance estimated by stroke volume-to-aortic pulse pressure ratio in humans. *Am. J. Physiol*. 1998; **274**(2 Pt 2):H500–H505.

47. J. Bermejo, The effects of hypertension on aortic valve stenosis. *Heart* 2005; **91**(3):280–282.

48. R. E. Mates and R. M. Judd, Models for coronary pressure-flow relationships. In: Sideman S., Beyar R., ed., Interactive phenomena in the cardiac system. New York: Plenum Press, 1993: 153–161.

49. J. I. Hoffman and J. A. Spaan, Pressure-flow relations in coronary circulation. *Physiol. Rev.* 1990; **70**(2):331–390.

50. M. Arsenault, N. Masani, G. Magni, J. Yao, L. Deras, and N. Pandian, Variation of anatomic valve area during ejection in patients with valvular aortic stenosis evaluated by two-dimensional echocardiographic planimetry: Comparison with traditional Doppler data. *J. Am. Coll. Cardiol*. 1998; **32**(7):1931–1937.

51. A. J. Fenlon and T. David, Numerical models for the simulation of flexible artificial heart valves: part I–computational methods. *Comput. Methods Biomech. Biomed. Engin*. 2001; **4**(4):323–339.